A transgenic mouse for *in vivo* detection of endogenous labeled mRNA

Timothée Lionnet[1,2], Kevin Czaplinski[1,5], Xavier Darzacq[3], Yaron Shav-Tal[4], Amber L Wells[1,5], Jeffrey A Chao[1], Hye Yoon Park[1,2], Valeria de Turris[1], Melissa Lopez-Jones[1] & Robert H Singer[1,2]

Live-cell single mRNA imaging is a powerful tool but has been restricted in higher eukaryotes to artificial cell lines and reporter genes. We describe an approach that enables live-cell imaging of single endogenous labeled mRNA molecules transcribed in primary mammalian cells and tissue. We generated a knock-in mouse line with an MS2 binding site (MBS) cassette targeted to the 3′ untranslated region of the essential β-actin gene. As β-actin–MBS was ubiquitously expressed, we could uniquely address endogenous mRNA regulation in any tissue or cell type. We simultaneously followed transcription from the β-actin alleles in real time and observed transcriptional bursting in response to serum stimulation with precise temporal resolution. We tracked single endogenous labeled mRNA particles being transported in primary hippocampal neurons. The MBS cassette also enabled high-sensitivity fluorescence *in situ* hybridization (FISH), allowing detection and localization of single β-actin mRNA molecules in various mouse tissues.

The mRNA molecule is the first intermediate of gene expression[1]. At every stage of its lifetime it is regulated both in space and time: transcription at the gene locus[2], export through the nuclear pore[3], diffusion and transport through the cytoplasm that in some cases result in localization of mRNA[4] and eventually decay, perhaps in specialized bodies[5]. These types of regulation are involved in many biological processes and diseases[6]. To completely understand the regulation of gene expression in physiological conditions as well as in the context of disease, ideally one would visualize single mRNA molecules in real time and over their lifetime in a living organism.

Such an experiment has been out of reach because it has not been possible to follow specific mRNAs transcribed from genes in their endogenous genomic context in primary cells or tissues. Therefore, the vast majority of our knowledge about mRNA regulation is derived from cultured cells. In cell culture, imaging of various stages of the mRNA life cycle has been possible using fluorescence microscopy techniques such as fluorescence recovery after photobleaching, fluorescence correlation spectroscopy or widefield microscopy[7]. These are particularly powerful when coupled with the *in vivo* mRNA imaging approach using the MS2 system[8]. In this technique, a sequence derived from the bacteriophage MS2 genome is inserted into a gene of interest. When transcribed, the RNA immediately folds into a hairpin that forms the MS2 binding site (MBS) for the bacteriophage MS2 capsid protein (MCP). When cells express both a gene of interest carrying the MBS and a fusion of MCP with a fluorescent protein (MCP-FP), mRNAs are fluorescently labeled from the moment they are transcribed (**Fig. 1a**). Insertion of multiple MBS copies (24 copies) increases the signal-to-noise ratio so that single mRNAs can be amplified over the background of freely diffusing MCP-FPs[8].

The MS2 system has been used in various contexts, such as bacteria[9], yeast[8], amoeba[10], fruit fly[11] and mammalian cells[12–16]. These studies have yielded a wealth of information about transcription kinetics (such as on-off pulsing of gene expression or the dynamics of elongation, including pausing), the dynamics of mRNA-protein complexes (mRNPs) and their intracellular localization. So far the MS2 system has only been applied to higher eukaryotes in the context of artificial reporter genes, usually inserted in many copies (10–1,000 copies) within a random locus[17]. Imaging artificial reporters in live cultured cells constitutes a useful experimental model but presents some limitations. In those systems consisting of many copies of the same gene, it is not possible to extract events happening at the single-gene level owing to the unsynchronized interactions taking place at the other genes in the locus. A recent improvement of the technique makes it possible to specifically insert single gene copies into the genome of a host cell line[18]. However, reporter genes might be prone to regulation artifacts. Notably, the use of immortalized cell lines introduces an unknown factor in the analysis of gene expression, in which regulatory events such as cell cycle controls are overshadowed by the transformed phenotype[19]. Finally, these systems do not permit the study of mRNA expression in primary cells or in tissue. As improvements in microscopy techniques

[1]Department of Anatomy and Structural Biology, Albert Einstein College of Medicine, Bronx, New York, USA. [2]Gruss Lipper Biophotonics Center, Albert Einstein College of Medicine, Bronx, New York, USA. [3]Institut de Biologie de l'Ecole Normale Supérieure, Centre National de la Recherche Scientifique Unité Mixte de Recherche 8197, Paris, France. [4]The Mina and Everard Goodman Faculty of Life Sciences & Institute of Nanotechnology and Advanced Materials, Bar-Ilan University, Ramat Gan, Israel. [5]Present addresses: Department of Biochemistry and Cell Biology, Center for Nervous Systems Disorders, Stony Brook University Stony Brook, New York, USA (K.C.) and Department of Medicine, Albert Einstein College of Medicine, Bronx, New York, USA (A.L.W.). Correspondence should be addressed to R.H.S. (robert.singer@einstein.yu.edu).

RECEIVED 23 SEPTEMBER 2010; ACCEPTED 10 DECEMBER 2010; PUBLISHED ONLINE 16 JANUARY 2011; DOI:10.1038/NMETH.1551

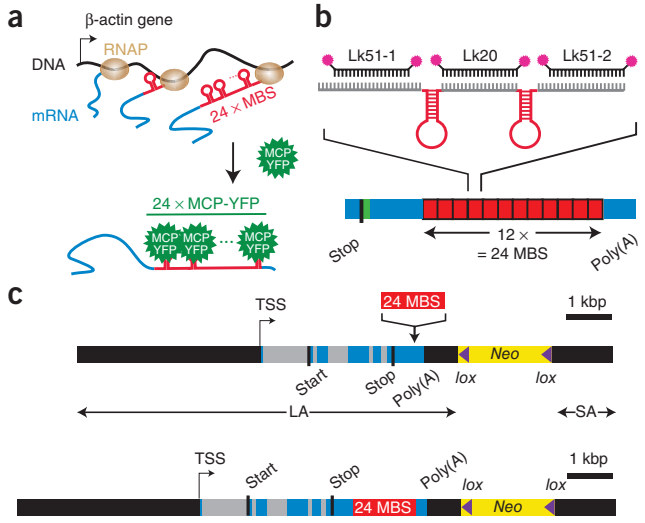

Figure 1 | Schematic of the *Actb*-MS2 system for live-cell imaging. (**a**) As the gene is transcribed by the RNA polymerase (RNAP), the RNA hairpins form and get bound by the coexpressed MCP-YFP. (**b**) In the MBS cassette, a unit containing two MBS sequences and the intervening linkers is repeated 12 times, resulting in 24 MBSs. We designed three FISH probes (named Lk51-1, Lk20 and Lk51-2) that bind each unit at the indicated positions. The MBS array is inserted downstream of the zip code regulatory region (green). (**c**) In the construct (top), the long homology arm (LA) encompasses the full *Actb* gene, including a region 4 kbp upstream of the transcription start site (TSS); the positions of the exons (blue), introns (gray), start and stop codon, and polyadenylation site (poly(A)) are indicated. The short homology arm (SA) extends 1.3 kbp downstream of the *Neo* cassette (yellow) flanked by the two *lox* sites (purple triangles). The 24× MBS cassette (red) is inserted in the 3′ UTR in the sixth exon. The resulting genomic locus in the *Actb*–MBS mouse is shown on the bottom.

lead to improvements in the ability to image in living tissue, gene reporters will be necessary to monitor expression, for instance, of disease-related defects.

The next step in understanding mRNA regulation in its native state is to apply the MS2 approach to a single endogenous gene in a multicellular organism. We generated a mouse that carries MBS repeats in the 3′ untranslated region (UTR) of both β-actin (*Actb*) alleles. We show that in addition to its use for live-cell imaging, the repeated MBS stem-loops provide an efficient target for high-sensitivity fluorescence *in situ* hybridization (FISH) in any tissue. We present a method to perform live-cell imaging in any cell type, by isolating the desired cells and by also expressing an MCP-FP either by transfecting a plasmid containing the *MCP-FP* gene or by stably integrating the MCP-FP coding sequence in the genome using lentivirus infection. We demonstrate the utility of this approach using the examples of mouse embryo fibroblasts (MEFs) and primary neuronal cell lines. This illustrates how single-gene kinetics in native cells can reveal details of the molecular mechanisms characteristic of different cell types. The *Actb-MBS* mouse offers a vast potential for imaging the lifecycle of an endogenous gene in its native environment, at the single-molecule level.

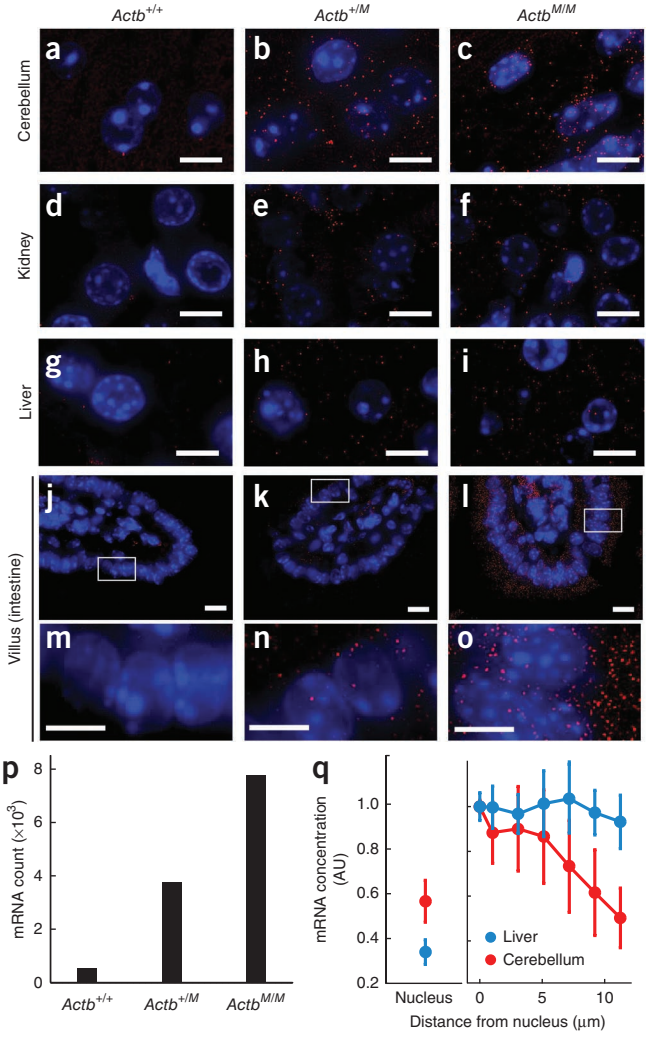

Figure 2 | RNA FISH in sections from various tissues. (**a**–**o**) Merge of DAPI signal (blue) and Cy5 fluorescence from three FISH probes targeting the MBS cassette (red; bandpass data) in the indicated tissues from the indicated strains. Scale bars, 10 μm (**a**–**l**), 5 μm (**m**–**o**; magnification of boxed areas in **j**–**l**). (**p**) Quantification of the *Actb-MBS* allele expression (number of spots counted) in the cerebellum after thresholding the FISH signal. (**q**) Average mRNA concentration inside the nucleus (left) and outside the nucleus, displayed as a function of the distance from the nuclear boundary (right). Both concentrations were normalized to their value at the nucleus boundary. AU, arbitrary units.

RESULTS

Generation of a homozygous *Actb-MBS* mouse

We used the *Actb* gene to test the feasibility of an 'MBS mouse'. *Actb* mRNA is an essential, ubiquitous, highly expressed[20], long-lived mRNA[21]. *Actb* mRNA is known to localize to the leading edge of fibroblasts, a process involved in maintaining cell polarity[22]. The understanding of this localization mechanism is important, as enhanced localization is correlated with persistent motility and decreased metastasis[6]. *Actb* mRNA is transcribed at a basal level in dividing cells, but its transcription can also be induced in response to serum addition[20]. Therefore it is a good model to study both the regulation of a constitutively expressed gene and the transcriptional response to environmental cues.

Mouse *Actb* consists of six exons spanning 3.5 kilobase pairs (kbp) on chromosome 5 and codes for the 375-amino-acid β-isoform of actin protein. The MBS motif can, in principle, either be introduced into the 5′ UTR or the 3′ UTR of the gene. A large number of MBS repeats increases the signal to improve detection

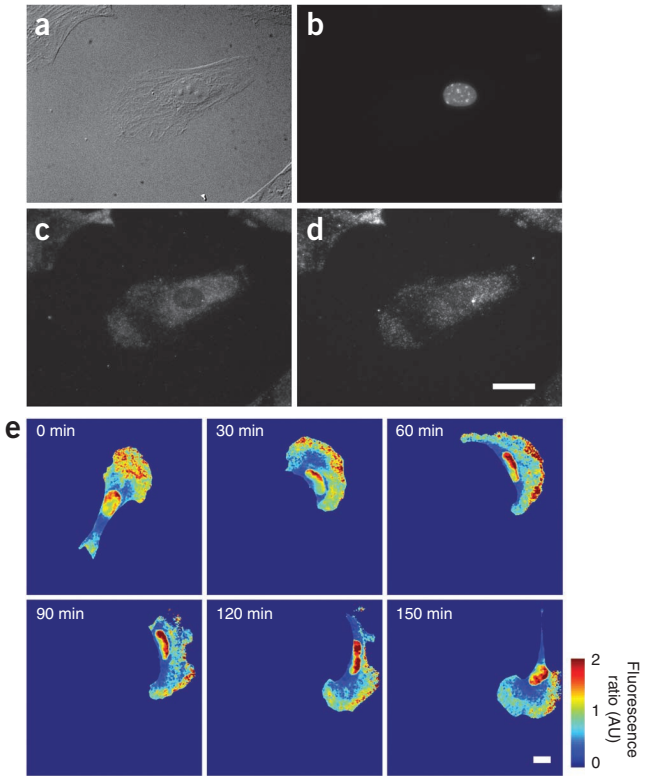

Figure 3 | *Actb* mRNA localizes to the leading edge of primary fibroblasts isolated from MBS mice. (**a**–**d**) Differential interference contrast image (**a**), DAPI-stained image (**b**), FISH with Cy3-labeled probes to the *Actb* coding region (**c**) and FISH with Cy5-labeled probes to the MBS cassette. (**d**) Scale bar, 10 μm. (**e**) Time-lapse images of a primary fibroblast migrating on a fibronectin substrate. Cells were infected with lentivirus that expresses NLS-MCP-GFP, and stained with membrane-permeant red cytoplasmic dye. Color bar, NLS-MCP-GFP fluorescence normalized by the red cytoplasmic dye intensity to account for the cell volume. AU, arbitrary units. Scale bar, 20 μm.

over a background of free fluorescent protein. We inserted the 1.2-kbp cassette containing 24 repeats of the MBS motif 441 bp downstream of the stop codon and after the zip code, a *cis*-regulatory sequence important for mRNA localization[23] (**Fig. 1b**,**c**). We linearized a construct carrying the modified gene and a *lox*-flanked neomycin resistance (*Neo*) cassette and electroporated it into embryonic stem cells (ESCs). After screening by PCR, we transfected the ESC clones containing this insert with a plasmid encoding the MCP-GFP protein to verify the correct expression of the transgene and to ensure that single-gene detection was feasible (data not shown). We used these ESC lines to generate chimeric mice, mated these chimeras and screened them for germline transmission to create knock-in mice (Ingenious Targeting Laboratory Inc.). Homozygous knock-in mice were viable and fertile, indicating that the presence of the MBSs was not notably deleterious.

We first verified that the transgene expressed the expected *Actb-MBS* mRNA. On a northern blot, the *Actb-MBS* mRNA was a single band with the expected shift in migration owing to the insertion of the MBSs (**Supplementary Fig. 1**). RNA isolated from various tissues expressed the complete mRNA containing MBSs in all tissues examined (**Supplementary Fig. 1**).

FISH imaging of *Actb* mRNA in tissue

In addition to its potential for live-cell imaging, the MBS array provides a target sequence optimized for detection by FISH. A mixture of three different probes complementary to the linker regions within the MBS repeats can potentially bind to 36 sites on the mRNA, providing strong signal amplification for detection in tissue sections (**Fig. 1b**). To test this, we sectioned paraffin-embedded tissue and performed RNA FISH using the MBS probes (**Fig. 2**). In both heterozygous ($Actb^{+/M}$ in which the superscript *M* refers to the *Actb-MBS* allele) and homozygous ($Actb^{M/M}$) tissue, we observed diffraction-limited particles, but observed no such particles in the wild-type ($Actb^{+/+}$) case (**Fig. 2a**–**o**), indicating that these signals correspond to *Actb–MBS* mRNA particles. To test the potential of the technique to quantify expression across tissue, we counted single mRNA particles in the cerebellum (**Fig. 2p**). We found as expected that the heterozygous mice expressed about 50% less *Actb-MBS* mRNA than the homozygous mice. Although *Actb* mRNA localization to the leading edge of cultured fibroblasts is well documented[22] (**Fig. 3**), what happens in tissue is still unclear. Using the MBS FISH probes, we quantified the spatial variation in *Actb-MBS* mRNA concentration within the liver and the cerebellum (**Fig. 2q**). The nuclear *Actb-MBS* mRNA concentration was on average lower than that outside of the nucleus, which probably reflects the difference between the time scales of transcription and export (few minutes[15]) and the lifetime of the *Actb* mRNA (few hours). We observed that the concentration of mRNA decreased with increasing distance from the nucleus in the cerebellum. This was not the case in liver tissue (**Fig. 2c**,**i**,**q**). This demonstrates the potential of our technique to quantitatively assess the spatial variations of mRNA concentration, an element that is crucially needed to establish a complete picture of gene expression *in vivo*. The probes targeted at the MBS cassette provided a much higher RNA FISH signal-to-noise ratio than a set of probes complementary to the *Actb* coding sequence. This demonstrates that in addition to its live-cell applications, the MBS sequence constitutes a unique FISH signal enhancing tag for detecting *Actb* transcription sites[24] as well as mRNP particles in mouse tissue, opening avenues for studying *Actb* mRNA regulation at the organ level.

Live-cell imaging in mouse-derived cell lines

Any primary cell from the mouse is amenable to live-cell imaging, which is a major advantage of the present technique over cell-line–based methods. Here we present applications to two cell types: fibroblasts and primary neurons. The fibroblast cell line we used has been used to study the export of single mRNA particles through nuclear pores with nanometer resolution[25].

We prepared embryonic day 14 (E14) MEFs from heterozygous and homozygous knock-in embryos and immortalized them using SV40 T antigen. We used the immortalized MEF lines to stably express MCP-YFP fusion protein with a nuclear localization sequence (NLS) (NLS-MCP-YFP). The presence of the NLS resulted in maintenance of a high NLS-MCP-YFP concentration in the nucleus and depletion of the cytoplasmic background of unbound NLS-MCP-YFP. This ensured the mRNA was bound by fluorescent NLS-MCP-YFP as soon as it was transcribed and that single molecules would be visible in the cytoplasm as there would be no unbound NLS-MCP-YFP to decrease the contrast. We isolated several cell lines stably expressing varying amounts of NLS-MCP-YFP

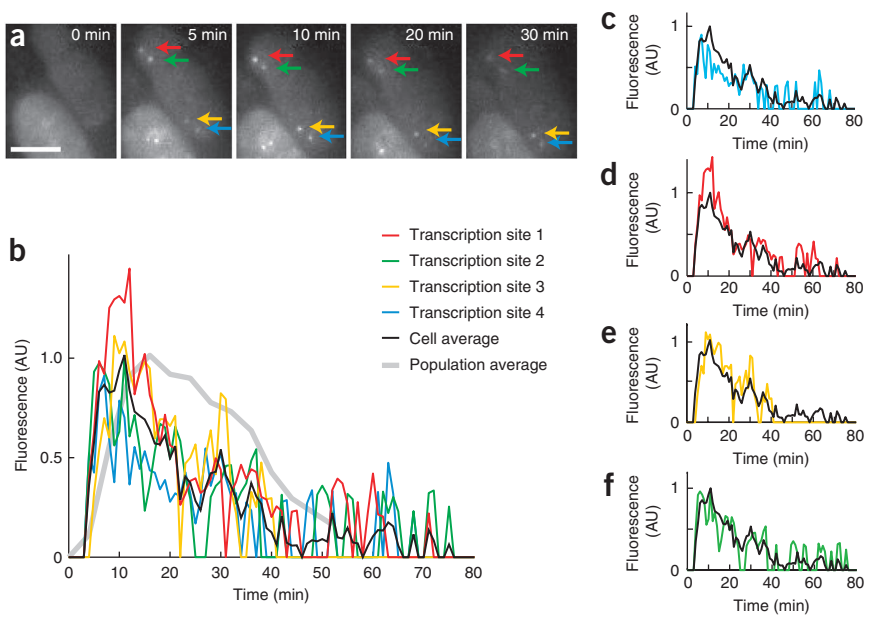

Figure 4 | Live-cell imaging of serum response in MBS immortalized MEFs. (**a**) Images of immortalized MEFs (tetraploids) during serum response taken at indicated times after serum addition (maximum intensity projections of *z*-dimension stacks). At 0 min, no transcriptional activity was detected, and at subsequent time points all four transcription sites appeared as bright nuclear spots (arrows). Scale bar, 5 μm. (**b**) Quantification of the fluorescence intensity at the transcription sites marked in **a**. Black, average response of the four alleles in **a**. Gray, average response over 11 cells. (**c**–**f**) Data from **b** shown separately for each allele. AU, arbitrary units.

and expressing MCP-YFP without the NLS. We karyotyped one cell line that we determined to be tetraploid, a common consequence of T-antigen immortalization[26] (**Supplementary Fig. 2**).

Homozygous cell lines expressed similar amounts of *Actb-MBS* mRNA and β-actin protein regardless of whether they coexpressed the NLS-MCP-YFP fusion protein (**Supplementary Fig. 1b**–**c**). β-actin protein levels were identical in all cell lines, although the homozygous mRNA levels were slightly lower than the wild-type cells (**Supplementary Fig. 3**). These results confirmed that neither the MBS cassette nor the NLS-MCP-YFP fusion protein prevented *Actb* expression. The γ-actin protein levels were also identical in all cell lines, indicating that there was no isoform compensation[27] (**Supplementary Fig. 1c**). Finally, we verified that the actin cytoskeleton had normal morphology in all cell lines by immunostaining MEFs with actin isoform–specific antibodies (**Supplementary Fig. 1d**).

To determine whether the MBS repeats affect transcription of *Actb*, we compared the numbers of *Actb* mRNA nascent chains at the gene loci of the wild-type and MBS-containing alleles in the heterozygous cell line. Quantitative RNA FISH showed that both alleles were transcribed with similar levels (**Supplementary Fig. 4**). In live homozygous primary fibroblasts, we detected transcription sites as two bright nuclear spots and mRNA particles as they moved in the cell (**Supplementary Movie 1**). We confirmed that *Actb-MBS* mRNA had the expected spatial localization to the leading edge of primary living fibroblasts[28] (**Fig. 3** and **Supplementary Fig. 5**), demonstrating that the repeats did not interfere with recognition of the zip-code sequence and hence affect mRNA localization.

Transcriptional bursting in MEFs after serum stimulation

We used the labeled MEFs to analyze serum-induced *Actb* mRNA transcription[20]. We cultured homozygous MEFs overnight in low serum. After addition of serum-containing medium, we imaged cells over time to follow *Actb* transcription. At the time of induction, we detected only fluorescence background in the nucleus owing to freely diffusing NLS-MCP-YFP (**Fig. 4a**). A few minutes after induction, four bright fluorescent spots corresponding to the *Actb* loci appeared in the nuclei and increased in intensity until ~10 min before gradually fading (**Fig. 4a**). RNA FISH probes targeted to both the *Actb* coding region and the MBS cassette co-localized with the bright NLS-MCP-YFP spots observed in the nucleus (**Supplementary Fig. 6**). Quantification of the intensities at each gene locus showed that the cells responded to serum by a burst of transcription that started after a few minutes and lasted for ~1 h (**Fig. 4b**). The four alleles, although subject to the same regulatory features (identical loci and intracellular cues) had varied responses (**Fig. 4c**–**f**). Although the alleles displayed a high synchrony in the initial minutes of the response, they quickly started to diverge and had largely uncorrelated behavior after 40 min. Different cells had distinct response curves that produced a broader response curve when averaged (**Fig. 4b**). The serum

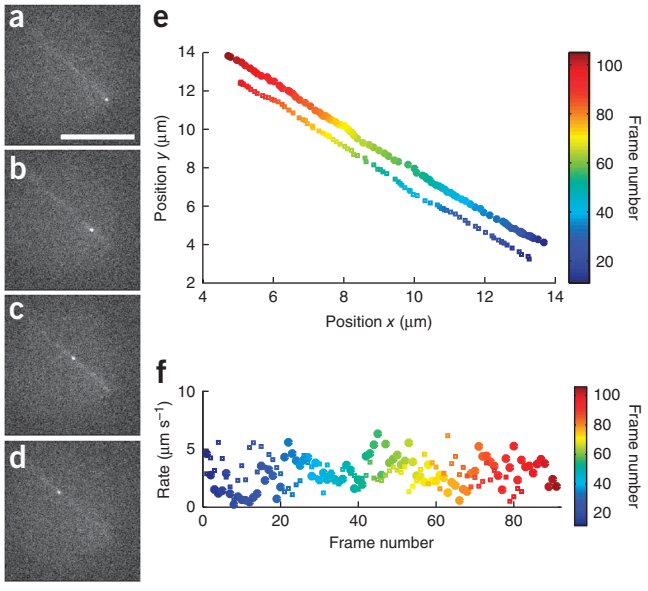

Figure 5 | Live-cell imaging of mRNP transport in primary hippocampal neurons. (**a**–**d**) Images of neurons transfected with a plasmid encoding MCP-YFP (imaged at 20 frames s^{-1}; shown images are 1 s apart) showing an mRNP moving unidirectionally along a neuronal process. Scale bar, 10 μm. (**e**) Trajectories of two particles (circles and squares) observed successively along the process shown in **a**–**d**. (**f**) Instantaneous rates for both mRNPs (averages ± s.e.m., 2.95 ± 0.14 μm s^{-1} (circles) and 2.90 ± 0.13 μm s^{-1} (squares)).

response kinetics observed here in the *Actb* MBS system were consistent with a previous RNA FISH analysis[20]. However, live-cell imaging offers many advantages such as finer time resolution than FISH and the possibility to follow the fate of each allele in an individual cell over long periods of time. Expression of the endogenous alleles will allow a rigorous evaluation of the intrinsic and extrinsic factors regulating *Actb* expression, a model essential constitutive gene, in its native state in a variety of tissues.

Actb mRNA transport in neurons

Owing to their extremely polarized structure, neurons provide an intrinsic challenge to gene expression: how, when and in what form do mRNAs reach the synapses where they undergo localized translation to strengthen specific synapses required for the stable interactions required for memory? We isolated primary neurons from MBS mouse embryos and expressed the NLS-MCP-YFP. It was then possible to follow the motion of individual particles in neuronal processes with high (20 frames s^{-1}) spatiotemporal resolution (**Fig. 5a–d** and **Supplementary Movies 2** and **3**). We observed several qualitatively different particle behaviors: unidirectional motion (anterograde and retrograde sometimes on the same process, **Supplementary Movies 4** and **5**), bidirectional motion (one particle moving in one direction then back in the opposite direction, **Supplementary Movie 6**), branching motion (one particle moving from one branch of a process to another; **Supplementary Movie 7**) or immobile particle (**Supplementary Movie 8**). Quantitative analysis of the tracks (**Fig. 5e**,**f**) yielded instantaneous transport rates in the 0.5–5 μm s^{-1} range, with averages around 3 μm s^{-1}. These rates are similar to the ones observed when tracking zip code–binding protein ZBP1 granules[29], a protein that binds *Actb* mRNA and is crucial for its localization. Previous work on granules has used transfected reporter genes to follow the movements of mRNAs in neurons, a process that inevitably leads to overexpression artifacts. This is the first detection of an endogenously expressed mRNA at its normal level and will allow for a more physiological analysis of the composition of the granules (are they single *Actb* mRNAs or clusters?) as well as details of their movements.

DISCUSSION

Labeling of endogenous *Actb* mRNA with the MBS cassette makes it possible to investigate how different tissues maintain a homeostasis of this structural protein. This approach is also a means to develop high-resolution, rapid imaging capabilities in tissue as single mRNA particles are visible in fixed tissue. Therefore it should be possible to record events of mRNA expression such as transport and localization in differentiating or regenerating tissues. This approach has several advantages over existing techniques: the gene studied is endogenous, in its native chromosome locus (including promoter, terminator and any other regulatory sequences); it is present at a single copy (hence imaging the activity at the locus truly reflects the activity of a single gene versus the average activity of many copies of the same gene in the case of a gene array); both alleles of the gene are amenable to imaging, which constitutes a useful system to study transcriptional regulation and variability; it is expressed in the mouse and therefore is amenable to studying gene expression in tissue or in any desired primary cell type. We illustrated the feasibility of the MBS label on a crucial housekeeping gene, *Actb*, without disrupting the mouse physiology. We anticipate that the approach presented here is applicable to any gene of interest.

In addition to the increased sensitivity, we demonstrated in tissue FISH and live-cell experiments, the Actb-MBS mouse can be used for other developments. The obvious application is intravital mRNA imaging. The mouse we described here contains only the protein-binding site, but the complete system (*Actb-MBS* coexpressed with a fusion MCP-FP) can be obtained by various means. For example, one could cross the Actb-MBS mouse with a mouse expressing an MCP-FP fusion or locally infect the Actb-MBS mouse with viruses designed to express the MCP-FP. Intravital studies of *Actb* mRNA localization could lead to better understanding the role of *Actb* mRNA localization in cancer and metastasis[6]. Also of interest is the study of the modes of transcription regulation at the level of the organism, a crucial feature, for example, during development[30].

Finally, the *Actb*–MBS mouse also provides a powerful tool for biochemistry. Taking advantage of the 24 high-affinity binding sites, one should be able to isolate the *Actb* mRNA with a very high signal-to-noise ratio. This will make it possible to identify the binding partners of *Actb* mRNA in various tissues.

We anticipate that the *Actb-MBS* mouse line will be a valuable tool to study the mRNA lifecycle using multiple, complementary approaches (from fixed- and live-cell imaging to biochemistry). In addition, our method can be adapted to study the expression of any gene of interest in its natural context.

METHODS

Methods and any associated references are available in the online version of the paper at http://www.nature.com/naturemethods/.

Note: Supplementary information is available on the Nature Methods website.

ACKNOWLEDGMENTS

We thank D. Ron (Skirball Institute of Biomolecular Medicine) for providing the SV40 large T antigen plasmid (pBSSVD2005) and the MEF immortalization protocol, C. Chaponnier (Université de Genève) for the gift of antibodies, C. Montagna for assistance in karyotyping and R.S. Sellers for assistance in tissue examination. The phage-UbC RIG vector for lentiviral expression was a generous gift from G. Mostoslavsky and G. Vainer (Harvard University). Microscopy equipment for the live-cell imaging experiments was provided by the Gruss Lipper Biophotonics Center. T.L. was supported by a Human Frontier Science Program long-term fellowship. This work was supported by US National Institutes of Health (GM84364, 86217 and EB2060 to R.H.S.), the Jane Stern Lebell Family Fellowship of Bar-Ilan University to Y.S.-T., and US-Israel Binational Science Foundation to Y.S.-T. and R.H.S. H.Y.P. is supported by National Research Service awards (F32-GM087122). A.L.W. is supported by a development grant from the Muscular Dystrophy Association (MDA68802).

AUTHOR CONTRIBUTIONS

T.L. performed the biochemistry experiments, the tissue FISH imaging, serum response live-cell imaging, and quantitative mRNA FISH, analyzed the data and wrote the paper. K.C. generated cell lines and performed the neuron live-cell imaging. X.D. and Y.S.-T. generated the mouse line. A.L.W. performed FISH mRNA localization experiments. J.A.C. performed the serum response live-cell imaging. H.Y.P. performed the live-cell localization experiments. V.d.T. generated cell lines. M.L.-J. performed the biochemistry experiments. R.H.S. consulted on the research and helped write the paper.

COMPETING FINANCIAL INTERESTS

The authors declare no competing financial interests.

Published online at http://www.nature.com/naturemethods/.
Reprints and permissions information is available online at http://npg.nature.com/reprintsandpermissions/.

1. Orphanides, G. & Reinberg, D. A unified theory of gene expression. *Cell* **108**, 439–451 (2002).
2. Sexton, T., Schober, H., Fraser, P. & Gasser, S.M. Gene regulation through nuclear organization. *Nat. Struct. Mol. Biol.* **14**, 1049–1055 (2007).
3. Terry, L.J., Shows, E.B. & Wente, S.R. Crossing the nuclear envelope: hierarchical regulation of nucleocytoplasmic transport. *Science* **318**, 1412–1416 (2007).
4. Czaplinski, K. & Singer, R.H. Pathways for mRNA localization in the cytoplasm. *Trends Biochem. Sci.* **31**, 687–693 (2006).
5. Garneau, N.L., Wilusz, J. & Wilusz, C.J. The highways and byways of mRNA decay. *Nat. Rev. Mol. Cell Biol.* **8**, 113–126 (2007).
6. Shestakova, E.A., Wyckoff, J., Jones, J., Singer, R.H. & Condeelis, J. Correlation of beta-actin messenger RNA localization with metastatic potential in rat adenocarcinoma cell lines. *Cancer Res.* **59**, 1202–1205 (1999).
7. Darzacq, X. *et al.* Imaging transcription in living cells. *Annu. Rev. Biophys.* **38**, 173–196 (2009).
8. Bertrand, E. *et al.* Localization of ASH1 mRNA particles in living yeast. *Mol. Cell* **2**, 437–445 (1998).
9. Golding, I., Paulsson, J., Zawilski, S.M. & Cox, E.C. Real-time kinetics of gene activity in individual bacteria. *Cell* **123**, 1025–1036 (2005).
10. Chubb, J.R., Trcek, T., Shenoy, S.M. & Singer, R.H. Transcriptional pulsing of a developmental gene. *Curr. Biol.* **16**, 1018–1025 (2006).
11. Jaramillo, A.M., Weil, T.T., Goodhouse, J., Gavis, E.R. & Schupbach, T. The dynamics of fluorescently labeled endogenous gurken mRNA in *Drosophila*. *J. Cell Sci.* **121**, 887–894 (2008).
12. Shav-Tal, Y. *et al.* Dynamics of single mRNPs in nuclei of living cells. *Science* **304**, 1797–1800 (2004).
13. Janicki, S.M. *et al.* From silencing to gene expression: real-time analysis in single cells. *Cell* **116**, 683–698 (2004).
14. Darzacq, X. *et al.* In vivo dynamics of RNA polymerase II transcription. *Nat. Struct. Mol. Biol.* **14**, 796–806 (2007).
15. Mor, A. *et al.* Dynamics of single mRNP nucleocytoplasmic transport and export through the nuclear pore in living cells. *Nat. Cell Biol.* **12**, 543–552 (2010).
16. Ben-Ari, Y. *et al.* The life of an mRNA in space and time. *J. Cell Sci.* **123**, 1761–1774 (2010).
17. Darzacq, X., Singer, R.H. & Shav-Tal, Y. Dynamics of transcription and mRNA export. *Curr. Opin. Cell Biol.* **17**, 332–339 (2005).
18. Yunger, S., Rosenfeld, L., Garini, Y. & Shav-Tal, Y. Single-allele analysis of transcription kinetics in living mammalian cells. *Nat. Methods* **7**, 631–633 (2010).
19. Mayr, C. & Bartel, D.P. Widespread shortening of 3′UTRs by alternative cleavage and polyadenylation activates oncogenes in cancer cells. *Cell* **138**, 673–684 (2009).
20. Femino, A.M., Fay, F.S., Fogarty, K. & Singer, R.H. Visualization of single RNA transcripts *in situ*. *Science* **280**, 585–590 (1998).
21. Sharova, L.V. *et al.* Database for mRNA half-life of 19 977 genes obtained by DNA microarray analysis of pluripotent and differentiating mouse embryonic stem cells. *DNA Res.* **16**, 45–58 (2009).
22. Shestakova, E.A., Singer, R.H. & Condeelis, J. The physiological significance of beta-actin mRNA localization in determining cell polarity and directional motility. *Proc. Natl. Acad. Sci. USA* **98**, 7045–7050 (2001).
23. Kislauskis, E.H., Zhu, X. & Singer, R.H. Sequences responsible for intracellular localization of beta-actin messenger RNA also affect cell phenotype. *J. Cell Biol.* **127**, 441–451 (1994).
24. Capodieci, P. *et al.* Gene expression profiling in single cells within tissue. *Nat. Methods* **2**, 663–665 (2005).
25. Grunwald, D. & Singer, R.H. *In vivo* imaging of labelled endogenous beta-actin mRNA during nucleocytoplasmic transport. *Nature* **467**, 604–607 (2010).
26. Ray, F.A., Peabody, D.S., Cooper, J.L., Cram, L.S. & Kraemer, P.M. SV40 T antigen alone drives karyotype instability that precedes neoplastic transformation of human diploid fibroblasts. *J. Cell. Biochem.* **42**, 13–31 (1990).
27. Dugina, V., Zwaenepoel, I., Gabbiani, G., Clement, S. & Chaponnier, C. β- and γ-cytoplasmic actins display distinct distribution and functional diversity. *J. Cell Sci.* **122**, 2980–2988 (2009).
28. Lawrence, J.B. & Singer, R.H. Intracellular localization of messenger RNAs for cytoskeletal proteins. *Cell* **45**, 407–415 (1986).
29. Tiruchinapalli, D.M. *et al.* Activity-dependent trafficking and dynamic localization of zipcode binding protein 1 and beta-actin mRNA in dendrites and spines of hippocampal neurons. *J. Neurosci.* **23**, 3251–3261 (2003).
30. Boettiger, A.N. & Levine, M. Synchronous and stochastic patterns of gene activation in the *Drosophila* embryo. *Science* **325**, 471–473 (2009).

ONLINE METHODS

Generation of the knock-in mouse. We targeted the MBS cassette to the 3′ UTR of the mouse *Actb* gene, downstream of the zip code. We identified a suitable region containing appropriate restriction sites for integration of the 24× MBS cassette. We used a ~9.6-kb genomic region to construct the targeting vector that was first subcloned from a positively identified bacterial artificial chromosome (BAC) clone containing the mouse *Actb* gene. We designed the region such that the long homology arm (LA) includes the full *Actb* gene, extending from ~4 kbp upstream of the *Actb* transcription start site to ~750 bp downstream of the end of the last exon. The short homology arm (SA) extends 1.3 kb 3′ downstream of the *Neo* cassette (**Fig. 1c**). The 1.3-kbp MBS cassette is inserted 441 bp downstream to the stop codon.

The generation of the targeting vector, the ESCs and the heterozygous mice was performed by Ingenious Targeting Laboratory Inc. We digested the MBS cassette on both ends using MluI and ligated the product into the MluI site of a vector containing the *loxP*-flanked Neo cassette. We synthesized a PCR fragment from the genomic DNA using primers containing MluI and AscI sites to generate the sequence between the site of the MBS cassette insertion and the site of the *Neo* cassette insertion, respectively. We ligated it into the vector between the MBS and the *Neo* cassettes. We excised the region including the MBS repeats, the intervening genomic sequence and the *Neo* cassette using BsiWI and ligated it into the targeting construct. The exact genomic sequence was restored except for the insertion of the MS2 repeats and the floxed *Neo* cassette at the locations described above (**Fig. 1c**). We confirmed the targeting vector by restriction analysis and sequencing.

The targeting vector was linearized and transfected by electroporation into 129SVev ESCs. After selection in G418, we expanded surviving clones for PCR analysis to identify recombinant ESC clones (**Supplementary Fig. 7**). We obtained three stable ESC clones and verified the expression of the *Actb-MBS* by RNA FISH and by co-expression of MCP-GFP in both undifferentiated and differentiated state. We injected the confirmed *Actb-MBS* (positive) ESC cells into foster mothers and obtained a chimeric litter (based on coat color). Two males showing 90% chimerism were mated with female mice, and 7 positive F1 germline mice (4 males, 3 females) were obtained from clone 3C-C3. We verified F1 mice by genotyping and PCR of the MS2 sequences, as well as RNA FISH in primary mice cells derived from mouse tissues. Experiments with mice were approved by the Institutional Animal Care and Use Committee of Albert Einstein College of Medicine (protocol 20100908).

Plasmids. We created an *NLS-MCP-YFP* gene using PCR. The final construct adds an NLS and an hemagglutinin (HA) tag to the N terminus of the previously reported construct MCP-YFP[31]. We cloned this expression cassette into the pHAGE-Ubc-RIG lentiviral vector[32] from which the DsRed-IRES-GFP fragment had been excised using NotI and ClaI. We used this plasmid to create recombinant lentiviral particles generating expression of NLS-MCP-YFP driven from the human ubiquitin C promoter in target cells.

Isolation of primary hippocampal neurons from mouse embryos. We isolated E18 mice from the pregnant female. We excised the hippocampus from the brain and placed it into sterile cold Hank's balanced salt solution (HBSS, without Mg^{2+}, without Ca^{2+} supplemented with 5 mM HEPES). We then dissociated tissue using a scalpel, resuspended it in 15 ml ice cold HBSS and centrifuged it (100*g* for 1 min). We resuspended the supernatant into 2 ml per brain of HBSS supplemented with 1:10 of 2.5% trypsin solution (Invitrogen) and incubated for 20 min at 30 °C. We added 1/9 volume of Ovomucid trypsin inhibitor (OMI; 10 mg ml^{-1} in PBS) and 1/19 volume of DNase I (100 mg; Sigma) resuspended in HBSS without Mg^{2+} or Ca^{2+} then sterile-filtered) and the tube was left to incubate 5 min at room temperature (22 °C). We resuspended the remaining tissue in DMEM with 10% FBS, further dissociated using a fire polished Pasteur pipette and allowed it to settle for 3 min (operation was repeated up to 8 times). We counted and deposited cells on polylysine-coated coverslips, allowed them to attach (1 h at 37 °C, 5% CO_2), and replaced the culture medium by fresh Neurobasal medium (Invitrogen) supplemented with 1× B27 (Gibco) 2 mM glutamax (Invitrogen), Primocin (Invivogen) and 25 µM glutamate. We then half-changed the medium every 3–4 d (omitting glutamate), supplementing with 10 µM cytosine arabinoside. To express NLS-HA-MCP-YFP in primary neurons, we applied lentiviral particles generated using the pHAGE vector to primary neurons by addition to the culture medium 1 d after plating. We maintained cells under standard neuron culture conditions and could see expression as early as 36 h after infection.

Isolation of MEF lines from mice. For the MEF lines, we isolated E14 mice from the pregnant female. We separated the head from the body and used it to genotype each embryo. We removed the dark cardiac tissue from the body and digested the body with trypsin-EDTA for 20 min. We plated MEFs isolated from each embryo separately into a 10-cm dish and grew them for 1 d in DMEM with 10% FBS and with antibiotics. We detached the cells with trypsin and seeded them into a culture dish for immortalization or froze them in 10% DMSO in DMEM with 10% FBS. To express NLS-MCP-GFP in primary MEFs, we seeded cells on the day of their isolation on a fibronectin coated Labtek chamber (Thermo Scientific) and incubated them with lentiviral particles generated using the pHAGE vector.

To immortalize MEFs, we transfected the cells with a plasmid expressing SV40 large T antigen (pBSSVD2005, gift of D. Ron) using Fugene 6 (Roche). We followed protocol: after transfection cells were grown to confluence and then serially passaged at high and low densities at least five times to select transformed cells. To stably express MCP-YFP or MCP-GFP, we created recombinant lentiviral particles using the phage UbC plasmid (described above) and used them to infect these cells according to existing protocols. We used infected cultures after several passages to create a highly enriched population of stably expressing cells by flow cytometry of MCP-YFP fluorescent cells. We later selected individual clones from the MCP-YFP–expressing cell lines.

Northern blotting. We scraped MEFs grown in DMEM with 10% FBS and 1% penicillin-streptomycin (pen-strep) from their dish. For tissue, we snap-froze tissue in liquid nitrogen and grinded it using a pestle and mortar. We then extracted total RNA using the RNeasy mini kit (Qiagen). We diluted 20 µg RNA in 50% formamide, denatured it 5 min at 65 °C, chilled it on ice and

then loaded it on a nondenaturing 1% agarose gel in 0.5× TBE. The RNA was transferred overnight onto an immobilon N+ membrane (Millipore). After UV-light cross-linking, we incubated the membrane 1 h at 37 °C in prehybridization solution (6× SSC, 50 mM $NaPO_4$ (pH 7.0), 5× Denhardt solution and 4% SDS). We generated random-primed DNA probes labeled with [γ-^{32}P]ATP (Perkin Elmer) using Klenow enzyme (Roche). We prepared the DNA templates by PCR of MEF cDNA for the wild-type *Actb* and *GAPDH* probes, and used a cleaved-out MBS insert for the MBS probe. We diluted the DNA probe in 10 ml pre-hybridization solution and incubated it with the membrane for 3 h at 37 °C. We washed the membrane twice 20 min at 37 °C in 7× SSC, 50 mM $NaPO_4$ (pH 7.0) and 1% SDS, and exposed it overnight to a storage phosphor screen before imaging on a Storm 860 phosphorimager (Molecular Dynamics).

RNA FISH. We performed RNA FISH on cultured cells to a protocol modified from previously published protocols[20,33]. The probes used were 50-mers of single-stranded DNA bearing each 4–5 fluorophores (probes are listed in **Supplementary Note 1**). We grew MEFs on coverslips in DMEM 10% FBS 1% pen-strep, then fixed them in 4% paraformaldehyde for 15 min at room temperature before washing and storing in PBSM (PBS supplemented with 5 mM $MgCl_2$) at 4 °C. Before hybridization, we permeabilized the cells 10 min in 0.5% triton X100 in PBS, then washed them in PBS 10 min, and incubated 10 min in prehybridization solution (50% formamide, 2× SSC, 2 mg ml^{-1} BSA, 0.2 mg ml^{-1} *Escherichia coli* tRNA and 0.2 mg ml^{-1} sheared salmon sperm DNA). We then hybridized the probes to the cells for 3 h in prehybridization solution supplemented with 10 ng DNA probe per locus per coverslip. We washed coverslips twice 20 min at 37 °C with prehybridization solution, then 10 min at room temperature in 2× SSC, and 10 min at room temperature in PBSM. We counterstained DNA with DAPI (0.5 mg l^{-1} in PBS). After a final wash in PBS, we mounted coverslips mounted on slides using ProLong gold reagent (Invitrogen). When 20-mer probes were used, we replaced the prehybridization solution by 10% formamide with 2× SSC, 2 mg ml^{-1} BSA, 0.2 mg ml^{-1} *E. coli* tRNA, 0.2 mg ml^{-1} sheared salmon sperm DNA and 10% dextran sulfate.

We performed RNA FISH in tissue sections following a published method[24]. Immediately after extraction from killed mice, we fixed the tissues in formalin overnight and paraffin-embedded them. We used 5-µm-thick sections for FISH. We incubated the sections at 55 °C for 30 min, then submitted them to a high pressure treatment (30 s at 125 °C, then 10 s at 90 °C under ~18 pounds per square inch) in decloaker reveal reagent (Biocare medical). After 5 min incubation in H_2O, we briefly rinsed the slides in H_2O and PBS. We incubated the sections 20 min at room temperature in 0.25% NH_4OH with 70% EtOH, 50 min at 4 °C in freshly prepared 0.5% $NaBH_4$ in PBS, then rinsed them in water and then PBS. We incubated the slides 10 min at room temperature in PBSM, then 3 times for 5 min in PBS and finally for 30 min in prehybridization solution. After a 2-h hybridization at 37 °C in a closed chamber, we washed the slides for 20 min at room temperature in prewarmed (37 °C) prehybridization solution, 20 min at room temperature in prewarmed (37 °C) 2× SSC, 20 min at room temperature in prewarmed (37 °C) 1× SSC, 15 min at room temperature in prewarmed (37 °C) 0.5× SSC and 5 min at room temperature in PBSM (all washes were performed on a slow rotary shaker). We counterstained the slides with 0.5 mg l^{-1} DAPI, washed them once in PBSM before mounting on coverslips using Prolong gold reagent (Invitrogen).

Immunofluorescence. As primary antibodies we used antibodies to β- and γ-actin isoforms (4C2F9H12/IgG1 and 2A3G8E2/IgG2b, respectively), a gift from C. Chaponnier[27]. We used as secondary antibodies, goat anti-mouse IgG1-FITC (Southern Biotech 1070-02) and anti-mouse IgG2b-TRITC (Southern Biotech 1090-03). We used a custom protocol[27]: we incubated cells in prewarmed L-15 supplemented with 10% FBS, then fixed them for 20 min at room temperature in 1% paraformaldehyde in L-15, 10% FBS. We washed cells twice in PBS, permeabilized the cells with methanol (–20 °C, 5 min) and rinsed in PBS. We then incubated the cells 1 h in the primary antibody mix (PBS supplemented with 3% 0.2-µm-filter-filtered BSA fraction V, antibodies diluted 1:100 β-actin; 1:200 γ-actin) at 37 °C in a closed chamber. We performed five rinses in PBS and incubated 1 h in the secondary antibody mix (PBS supplemented with 3% 0.2-µm-filter–filtered BSA fraction V, 1:50 Southern Biotech 1070-02 and 1:50 Southern Biotech 1090-03). After five rinses in PBS, we counterstained the DNA with 0.5 mg l^{-1} DAPI and mounted on slides using Prolong gold reagent (Invitrogen).

Western blotting. We used the following primary antibodies: β-actin (Sigma A1978), γ-actin (AB3265, Chemicon) and β-tubulin (Amersham N357), and secondary antibodies: donkey anti-mouse conjugated to IRDye 800 (Rockland 610-732-124) and donkey anti-sheep conjugated to Alexa Fluor 680 (Invitrogen A21102). We washed cells in ice-cold PBS and lysed them at room temperature for 2 min in 1 ml lysis buffer per 10-cm dish (50 mM Tris-HCl (pH 8.0), 150 mM NaCl, 1% NP40, 5 mM DTT, 1 mM PMSF and half a mini tablet protease inhibitor). We spun the lysate 15 min at 14,000*g* at 4 °C and loaded the supernatant on a Nupage 4–12% bis-tris gel using MOPS running buffer (Invitrogen). After transfer on a nitrocellulose membrane in Nupage transfer buffer (25 V for 1.5 h), we blocked nonspecific interactions by incubating the blot overnight at 4 °C in PBS supplemented with 5% nonfat dry milk. After that, we rinsed the membrane and incubated it for 1 h with the primary antibodies in PBS supplemented with 1% BSA (dilutions: 1:2,500 mouse anti–*Actb*; 1:5,000 mouse anti–β-tubulin). We then washed the blot 5 times 10 min in PBS with 0.3% Tween-20 before incubation for 30 min with the secondary antibody (1:10,000 in PBS with 1% BSA). We then washed the membrane 5 times in PBS with 0.3% Tween-20, before exposure on an Odyssey infrared imaging system (two-color detection). We quantified the bands intensities using ImageJ software (US National Institutes of Health).

Imaging. For immortalized cells, we plated homozygous MEFs expressing MCP-YFP on a 0.17 mm delta T dish (Bioptechs) and incubated 24 h in DMEM 10% FBS 1% pen-strep. We left cells to recover for 24 h and then starved them overnight. We replaced the medium by L-15 supplemented with the Oxyfluor oxygen scavenging system (Oxyrase) before the experiment. We placed the cells on an Olympus IX-71 microscope equipped with a 150×, 1.45 numerical aperture (NA) objective (Olympus) and a Cascade II camera (Photometrics). We maintained a constant temperature of 37 °C through the experiment using the Delta T chambers, a

doi:10.1038/nmeth.1551

heated lid and objective heater (Bioptechs). We imaged cells in three dimensions over time using a 200 nm *z*-dimension axis step size over a range of 4 μm every 4 min using a 488-nm argon laser for excitation of YFP fluorescence. We converted the three-dimensional *z*-dimension stacks into two-dimensional movies using a maximum intensity projection. For primary fibroblasts, we plated the cells on fibronectin-coated MatTek dishes (MatTek), infected with lentivirus to express NLS-MCP-GFP, and incubated them for 48 h in DMEM 10% FBS, 1% pen-strep. We stained the cells with 5 μM CellTracker Orange CMRA (Invitrogen) and replaced the medium with L-15 containing 10% FBS, 1% pen-strep and 1% oxyrase before the experiment. We used an Olympus IX-71 inverted microscope equipped with a 40×, 1.35 NA oil-immersion objective (Olympus) and electron-multiplying charge-coupled device (EMCCD) camera (Andor). We maintained the temperature at 37 °C using an environmental chamber (Precision Plastics). We excited GFP using a 488 nm line from an argon ion laser (Melles Griot) and CellTracker Orange CMRA using a 561 nm diode laser (Cobolt). For RNA FISH, we imaged the slides on an Olympus BX-61 microscope equipped with an X-cite 120 PC Mercury lamp (EXFO), a 100×, 1.4 NA objective (Olympus) and a Coolsnap HQ camera (Photometrics). For primary neurons, we changed neuron medium into Hibernate Low Fluorescence medium (BrainBits LLC) with 1× B27 supplement and 2 mM glutamax. After imaging, we restored cells to neurobasal medium with 1× B27, 2 mM glutamax with 1× primocin. We used the same imaging setup as that used for immortalized cells.

Image analysis. We performed spot detection and quantification from FISH and live-cell imaging using custom-designed interface description language (IDL) (ITT Visual Information Solutions) and Matlab (Mathworks) programs. We first detected high intensity pixels by two- or three-dimensional (when using three-dimensional image stacks) bandpass filtering the image (**Supplementary Fig. 8**) and then applied a threshold to the bandpassed image (we adjusted the threshold value depending on the quality of each individual image). We defined as spots the local maxima within a two-pixel radius of the pixels above threshold. We then automatically quantified the individual spots intensities the original image. To do so, we first corrected the intensity profile in a square region of interest (ROI) surrounding each spot for the local background, calculated as a the linear fit of the intensity versus position in the pixels adjacent to the ROI (we set the ROI size as three times the width of the point spread function (PSF)). Then we calculated the position and intensity of each spot using a two- or three-dimensional Gaussian mask fit of the PSF[34]. In the two-dimensional projections of the tissue FISH image stacks, we identified nuclei by either automatically thresholding or manually circling the DAPI signal. We then coarse-grained the image using 32 × 32 pixels (~2 × 2 μm) square bins. We counted the number of mRNA particles within each bin and computed the distance from that bin to the closest nucleus. We collected quantitative data over typically 100–150 cells.

31. Fusco, D. *et al.* Single mRNA molecules demonstrate probabilistic movement in living mammalian cells. *Curr. Biol.* **13**, 161–167 (2003).
32. Mostoslavsky, G., Fabian, A.J., Rooney, S., Alt, F.W. & Mulligan, R.C. Complete correction of murine Artemis immunodeficiency by lentiviral vector-mediated gene transfer. *Proc. Natl. Acad. Sci. USA* **103**, 16406–16411 (2006).
33. Raj, A., van den Bogaard, P., Rifkin, S.A., van Oudenaarden, A. & Tyagi, S. Imaging individual mRNA molecules using multiple singly labeled probes. *Nat. Methods* **5**, 877–879 (2008).
34. Thompson, R.E., Larson, D.R. & Webb, W.W. Precise nanometer localization analysis for individual fluorescent probes. *Biophys. J.* **82**, 2775–2783 (2002).